BMC Structural Biology

Research article

A role of proton transfer in peroxidase-catalyzed process elucidated by substrates docking calculations

Juozas Kulys*[1] and Arturas Ziemys[2]

Address: [1]Department of Enzyme Chemistry, Institute of Biochemistry, Mokslininku 12, Vilnius, 2600, Lithuania and [2]Department of Biology, Faculty of Natural Sciences Vytautas Magnus University, Vileikos 8, Kaunas, 3500, Lithuania

E-mail: Juozas Kulys* - jkulys@bchi.lt; Arturas Ziemys - a3arzi@vaidila.vdu.lt

*Corresponding author

Published: 28 August 2001

BMC Structural Biology 2001, **1**:3

Received: 5 July 2001

Accepted: 28 August 2001

This article is available from: http://www.biomedcentral.com/1472-6807/1/3

Abstract

Background: Previous kinetic investigations of fungal-peroxidase catalyzed oxidation of *N*-aryl hydroxamic acids (AHAs) and *N*-aryl-*N*-hydroxy urethanes (AHUs) revealed that the rate of reaction was independent of the formal redox potential of substrates. Moreover, the oxidation rate was 3–5 orders of magnitude less than for oxidation of physiological phenol substrates, though the redox potential was similar.

Results: To explain the unexpectedly low reactivity of AHAs and AHUs we made *ab initio* calculations of the molecular structure of the substrates following *in silico* docking in the active center of the enzyme.

Conclusions: AHAs and AHUs were docked at the distal side of heme in the sites formed by hydrophobic amino acid residues that retarded a proton transfer and finally the oxidation rate. The analogous phenol substrates were docked at different sites permitting fast proton transfer in the relay of distal His and water that helped fast substrate oxidation.

Background

Heme peroxidases are widespread in bacteria, fungi, plants and mammalians [1]. Therefore, peroxidase-catalyzed oxidation of organic compounds is a paramount electron transfer process in molecular biology. Phenols and anilines are generally recognized as substrates of the heme peroxidases (donor: H_2O_2 oxidoreductases EC 1.11.17). The peroxidases catalyze oxidation of the substrates by hydrogen peroxide or alkyl peroxides, usually but not always, via free-radical intermediates [1,2]. Non-phenolic compounds, such as indole-3-acetic acid, phenylenediamines, ferrocenes, phenothiazines, phenoxazines, have also been investigated as peroxidase substrates [2][3–5]. Steady-state kinetics of peroxidase action has been described as a ping-pong scheme with compound **I** and compound **II** formation [1].

The principal question in enzyme-catalyzed processes is the dependence of the reaction rate on the substrate and the enzyme active center structure. In peroxidase-catalyzed reactions it has been demonstrated that the reaction rate correlated with the substitution parameters of phenols [6]. The reactivity of the horseradish peroxidase toward phenols and non-phenolic substrates, i.e. indole-3-acetic acids, was compared on the basis of the thermodynamic driving force of the reaction [2]. These observations as well as kinetics of phenylenediamines, phenothiazines and phenoxazines oxidation revealed

that reactivity of peroxidases (at least within the same substrate type) were depend on redox properties of the compounds [2][3–6].

The peroxidase substrates investigated in [2,5] contained phenol or aniline structure in which *-OH* or *-NH* groups were conjugated with aromatic system. The oxidation rate of these substrates approached diffusion limit. However, during investigations of *N*-arylhydroxamic acids and *N*-aryl-*N*-hydroxyurethanes, containing redox core *Ar-N(OH)-COR* and *Ar-N(OH)-CO-OR*, unexpectedly low reaction rate has been established [7,8]. In order to explain the sharp difference of reactivity of phenols and non phenolic *N-OH* substrates in this study peroxidase kinetic results were compared with molecular parameters of substrates and their binding in the enzyme active centre.

Results

The structure of *N*-arylhydroxamic acids (AHAs) **1a-e, 2a-d, 3, 4, 5** and *N*-aryl-*N*-hydroxyurethanes (AHUs) **1–5** is shown in Figure 1 and Figure 2.

The investigated compounds are redox active in buffer solution at pH 4.0–10.0. Calculated formal oxidation-reduction potential of **AHA 1a** was 370 mV vs. SCE (612 mV vs NHE) at pH 8.5 [7]. It was dependent on the pH of the buffer solution (Figure 3). At least two transitions with pK_a3.7 ± 0.6 and with pK_a of 6.3 ± 0.1 were identified.

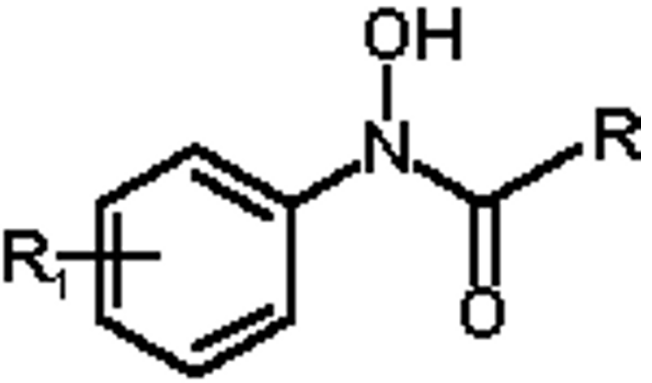

Figure 1
Structure of *N*-arylhydroxamic acids (AHAs). **AHA 1a:** R = CH_3 R_1 = H **AHA 1b:** R = CH_3 R_1 = *p*-NO_2 **AHA 1c:** R = CH_3 R_1 = *p*-CN **AHA 1d:** R = CH_3 R_1 = *p*-$COCH_3$ **AHA 1e:** R = CH_3 R_1 = *p*-OH **AHA 2a:** R = Ph R_1 = H **AHA 2b:** R = *p*-CH_3O-Ph R_1 = H **AHA 2c:** R = *p*-NO_2-Ph R_1 = H **AHA 2d:** R = *p*-CN-Ph R_1 = H **AHA 3:** R = 1-Napthyl R_1 = H **AHA 4:** R = CH_3 R_1 = *m*-NO_2-Ph **AHA 5:** R = Ph-C(O)N(OH)-Ph R_1 = H

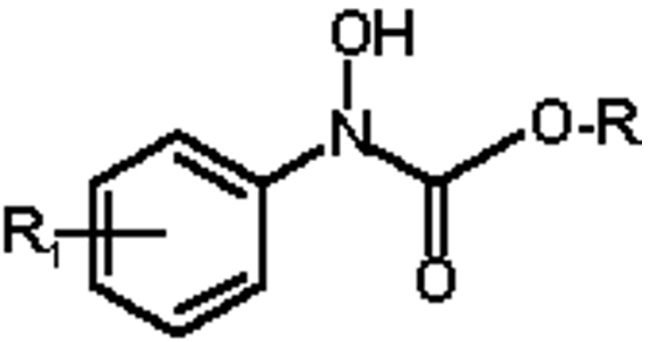

Figure 2
Structure of *N*-aryl-*N*-hydroxyurethanes (AHUs). **AHU 1:** R = CH_3 R_1 = H **AHU 2:** R = C_2H_5 R_1 = H **AHU 3:** R = *iso*-C_3H_7 R_1 = H **AHU 4:** R = Ph R_1 = H **AHU 5:** R = CH_3 R_1 = *p*-CN

pH dependence of redox potential has not been associated with acid-base dissociation of **AHA 1a** since absorption spectra didn't change at these pH values. Only nitro compounds, i.e.**AHA 1b** and**AHA 2c** changed absorption spectrum at different pH with an apparent pK_a of transitions 8.50 ± 0.1 and 8.0 ± 0.4, respectively [7]. The absorbance change was associated with heterolytic *NO-H* bond dissociation at alkaline pH.

The dependence of redox potential on pH could be explained by different oxidation mechanism. At pH larger than 7.5 the electrochemical conversion was associated with single electron transfer followed by fast proton-release (equations 1,2). At these pH values the process was not limited by proton transfer.

$$CH_3\text{-}CO\text{-}N(OH)\text{-}Ph \rightarrow CH_3\text{-}CO\text{-}N(O^{\bullet+}H)\text{-}Ph + e \quad (1)$$

$$CH_3\text{-}CO\text{-}N(O^{\bullet+}H)\text{-}Ph \rightarrow CH_3\text{-}CO\text{-}NO^{\bullet}\text{-}Ph + H^+ \quad (2)$$

In pH interval between pH 3.7–6.3 the oxidation proceeded by electron/proton transfer. At acidic pH (pH<3.7) **AHA 1a** oxidation was linked to electron transfer following the radical cation formation. The high redox potential of this conversion has been limited by slow proton transfer. The formal potentials of analyzed conversions were 368 ± 2, 481 ± 9 and 671 ± 170 mV (vs SCE), respectively. The role for proton transfer was confirmed during **AHA 1a** oxidation in methylene chloride. The oxidation of **AHA 1a** in this aprotic solvent proceeded at 1.0 –1.2 V.

The values of the formal redox potentials of all AHAs covered a range from 306 to 411 mV (Table 1).

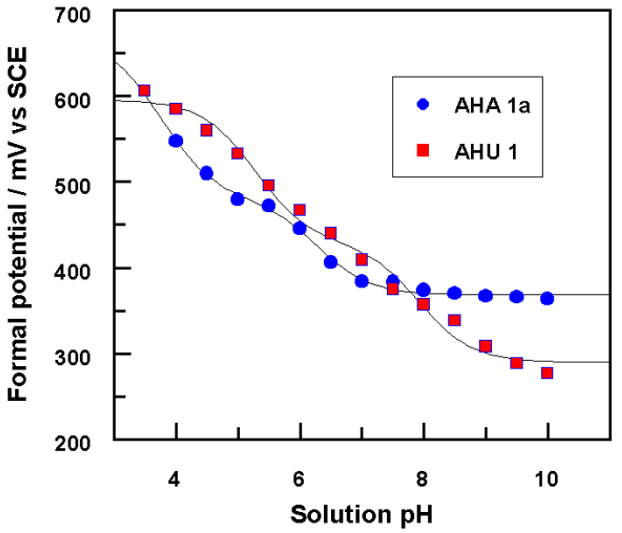

Figure 3
The dependence of formal redox potentials of **AHA 1a** and **AHU 1** on solution pH [7,8].

The calculated redox potentials of the substrates **AHU 1-4**changed in the range between 328 and 351 mV (Table 1). Formal potential of **AHU 1** was also dependent on pH (Figure 3). pK_a of transitions were 5.3 ± 0.2 and 7.9 ± 0.2. The pH dependence of transitions might be explained in the same manner as **AHA 1a** conversion (equations 1,2). The calculated values of formal potentials of each reaction were 595 ± 10, 430 ± 12 and 289 ± 8 mV.

Table 1: The redox potential (vs SCE) and oxidation constants of *N*-aryl hydroxamic acids and *N*-aryl-*N*-hydroxyurethanes at pH 8.5 and 25 °C [7,8].

Compound	E/mV	$k_{ox}/M^{-1}s^{-1}$
AHA 1a	370 ± 2	$(7.1 \pm 0.2) \cdot 10^3$
AHA 2a	375 ± 6	$(9.9 \pm 0.3) \cdot 10^4$
AHA 1b	411 ± 2	$(2.5 \pm 0.1) \cdot 10^5$
AHA 2b	313 ± 2	$(1.5 \pm 0.1) \cdot 10^5$
AHA 1c	406 ± 1	$(8.5 \pm 0.6) \cdot 10^3$
AHA 2c	375 ± 4	$(7.1 \pm 0.4) \cdot 10^4$
AHA 1d	393 ± 2	$(9.2 \pm 2.1) \cdot 10^4$
AHA 2d	391 ± 3	$(5.0 \pm 0.3) \cdot 10^4$
AHA 1e	369 ± 1	$(1.5 \pm 0.2) \cdot 10^7$
AHA 3	364 ± 2	$(8.3 \pm 0.6) \cdot 10^3$
AHA 4	403 ± 1	$(9.2 \pm 0.6) \cdot 10^3$
AHA 5	307 ± 2	$(8.7 \pm 0.4) \cdot 10^5$
AHU 1	345 ± 1	$(2.3 \pm 0.2) \cdot 10^4$
AHU 2	337 ± 2	$(7.5 \pm 0.5) \cdot 10^4$
AHU 3	328 ± 2	$(3.2 \pm 0.2) \cdot 10^4$
AHU 4	351 ± 4	$(4.2 \pm 0.2) \cdot 10^4$
AHU 5	396 ± 5	$(2.5 \pm 0.5) \cdot 10^4$

The steady state kinetics of the rCiP-catalyzed oxidation of substrates revealed that bimolecular constants of **AHAs** and **AHUs**oxidation, with exception of **AHA 1e** covered range from $8.3 \cdot 10^3$ to $8.7 \cdot 10^5$ $M^{-1}s^{-1}$ (Table 1). This rate is associated with compound **II** reduction [7,8]. Oxidation rate of **AHA1e** was 2100 times faster in comparison with **AHA 1a** (Table 1).

Discussion

A typical approach to evaluate structure activity relationship (SAR) in enzymatic redox reactions is the comparison of reaction rate with redox potential of substrates [2–6]. If electron transfer is predominantly chemically controlled, the reactivity of substrates should be related to the free energy of reaction (to the thermodynamic driving force) as it is the case of other electron transfer reactions [9]. However, only a tendency of the correlation of the *log* of bimolecular constants with the respective redox potentials could be observed for AHAs benzamides as predicted by electron transfer theory [9]. For acetamides an opposite tendency was found: the constant increased with increasing substrate potential. The reactivity of AHUs didn't correlate with redox potential too. In the attempt to find explanation of unusually low reactivity and independent reactivity to redox potential the docking of AHAs and AHUs in the active center of rCiP was calculated. The docking of the substrates in the active center of rCiP was calculated by taking from the bank the crystal structure of *Arthromyces ramosus* peroxidase (ARP) since these two enzymes vary only by one terminal amino acid [10].

The control calculations revealed that the docking of benzohydroxamic acid (BHA) completely fitted the crystallographic data, when the ARP structure was taken from ARP/BHA complex (HSR for further discussion) [11]. The calculations of **AHA 1a** in the HSR structure revealed two possible ways of the substrate complexation (Figure 4). The mean docking energies were -26.9 kJ mol^{-1} and -26.8 kJ mol^{-1} for the first and the second cluster, respectively. Thus about 73% of **AHA 1a** occupied by the first cluster. In both clusters the benzene ring was located at the entrance of the heme cavity and *N-OH* and *C=O* groups were placed inside the active center. In the first cluster methyl group and oxygen were connected to a water molecule, which was located at distal side of heme between the histidine residue and the iron atom. The structure of this cluster was almost identical to ARP/BHA cluster.

In the second cluster, **AHA 1a** was rotated 180° around *N*-phenyl axis and a little bit twisted while the water molecule interacted with the *C=O* group (Figure 4).

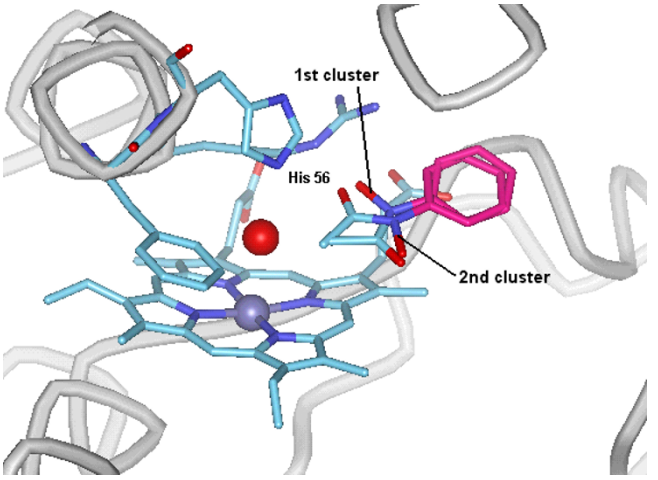

Figure 4
The docking of **AHA 1a** in the active center of HSR. The red ball shows a water molecule.

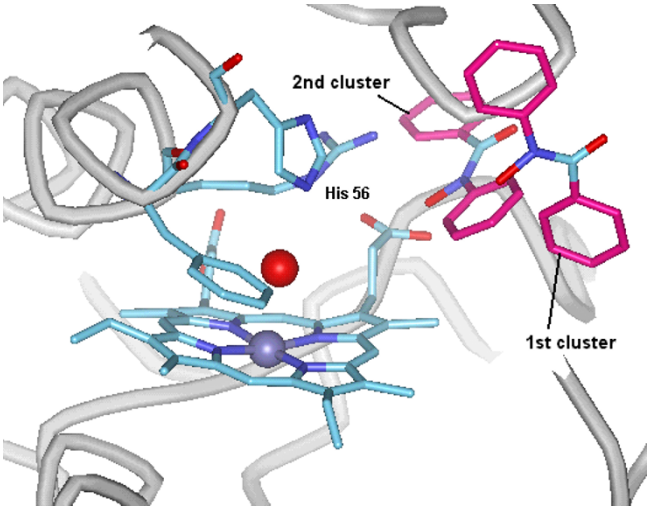

Figure 5
AHA 2a docking in the active center of HSR.

The calculations of **AHA 2a** docking revealed two complexation sites in the neighborhood of the heme (Figure 5). The largest amount (96.6%) of **AHA 2a** has been docked in a small pocket formed by of Pro 91 and Ile 153. A mean docking energy from 80% of these complexes was -30.7 kJ mol^{-1}. In the second type of clusters **AHA 2a** was located at the entrance to the heme. It had a mean docking energy of -25.6 kJ mol^{-1} and occupied 4.4% of all structures. In this cluster **AHA 2a** was located almost parallel to the heme plain and was placed in close proximity to methyl and propionic acid residues of the heme.

The calculations of the docking of **AHU 1** revealed that about 95% of the substrate combines in a small pocket at Pro 91 and Ile 153. The mean docking energy of these clusters changes from -21.87 to -26.77 kJ mol^{-1} or from -21.83 to -25.39 kJ mol^{-1}. The small amount of the substrate was also combined at the residues of Asp 98, Thr 99, and Lys 49. In this complex the *N*-aryl fragment was located at a distance of 14 Å from the heme and water molecule. The docking of **AHU4** produced 3 clusters near Pro 91 and Ile153 at the distal side of heme. A mean docking energy of these clusters was -29.54, -28.9 kJ mol^{-1} and -27.70 kJ mol^{-1}. The rest cluster was located in the heme pocket. The docking energy of this cluster was -26.90 kJ mol^{-1}. The *N*-aryl fragment was located at the distance of 4.72 Å from water molecule and *O*-aryl fragment was 3.73 Å from heme.

The calculations showed that other AHAs, with exception of **AHA 1e**, and AHUs were docked in the same sites as **AHA 1a**, **AHA 2a**, **AHU 1** and **AHU 4**. These sites were formed by hydrophobic amino acid residues. Dockings showed that hydrogen from *N-OH* group of **AHA 1a** and **AHU 1** does not form strong hydrogen bonds with polypeptide chain. In the case of **AHA 2a** and **AHU 4** *N-OH* group may form a weak hydrogen bong with Arg 52.

The docking of **AHA 1e** was different in comparison to the rest AHAs and AHUs (Figure 6).

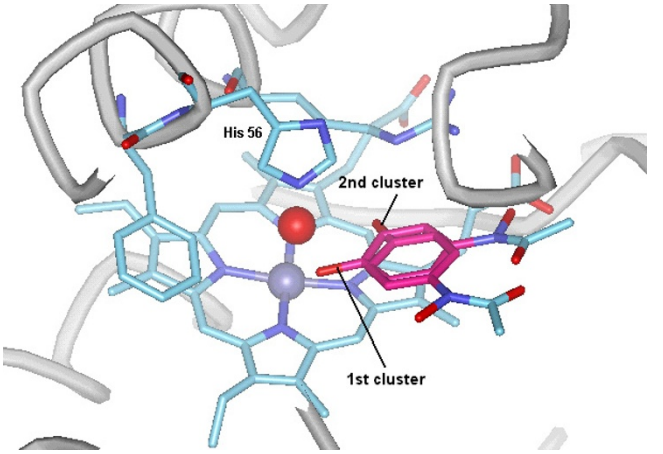

Figure 6
The docking of **AHA 1e** in the active center of HSR.

AHA 1e substrate was combined in such manner that hydroxyl group at *para* position of phenyl ring formed hydrogen bond with proximal His. Different **AHA 1e** docking in the active center and different reactivity of phenolic and *N-OH* substrates permits to hypothesize that peroxidase-catalyzed reactivity depends on proton transfer rate in the active center. The electrochemical investigations demonstrated that proton transfer rate de-

termined formal redox potential of the substrates in water solution. In acidic solutions or in aprotic non-polar solvent like methylene chloride the proton transfer was retarded and oxidation of substrate proceeded at high potential. The complexation of substrates in the hydrophobic site of the enzyme also retards proton transfer during oxidation. If proton transfer limits the reaction the local surrounding of *N-OH* group can be critical to the reaction rate. The combining of AHAs and AHUs in hydrophobic surrounding does not permit fast proton transfer. The larger reactivity of **AHA 2a** or benzamides may be explained by hydrogen bond formation with Arg 52 and facilitated proton transfer. The combining of **AHA 1e** in the site where proton transfer is fast due to hydrogen bonds relay to distal His and proximal water makes fast substrate oxidation.

The role of proton transfer in enzymatic oxidoreductase catalysis was described in many publications [12]. During *C-H* bond oxidation of specific substrates the proton is tunneling along the reaction coordinate and the rate of overall process depends on this process. Recent investigations of peroxidases catalysis permitted to make conclusions that proton transfer with participation of distal water molecule also plays an important role in peroxidases-catalyzed oxidation of physiological substrates. Recently Henriksen and co-workers proved that the oxidation of ferulic acid by plant peroxidase is accompanied by proton transfer with distal water molecule being involved into the process [13]. The conclusion was made that in the case of compound I reduction the final destination of proton was the distal histidine whereas ferryl oxygen was the proton acceptor in the case of compound II reduction. The detail analysis of roles of water made by Jones [14] permitted to hypothesize that presence or absence of "resident" water molecule at distal site of heme may switch between peroxidase and catalase activities.

Conclusions

The hypothesis formulated in this work states that docking of non-specific substrates may cause troubles of proton transfer relay formation in the active centre of peroxidases and may control the rate of the substrates oxidation if proton transfer is associated with the oxidation reaction. This hypothesis permits to explain unusually low activity of some type of substrates and opens possibilities for new substrates design. Although the experimental results are consistent with the docking calculations more directly target studies such as determination of ternary structure of peroxidase and substrate complex with cyanide are highly desirable.

Materials and Methods

The synthesis of the substrates and the methods used are described in [7,8]. Kinetic measurements were performed by using recombinant *Coprinus cinereus* peroxidase (rCiP) in [7,8].

Ab initio calculations of electronic structure and the energies of substrates were performed using a Gaussian 94W package [15]. Geometry optimization of the substrates was accomplished using HF (Hartree-Fock) theory and a 3–21G basis set. The optimized geometry of molecules was used for energies and charges calculations with a 6–31G basis set using RHF and B3PW91 (Density Functional Theory). The atom charges of molecules were calculated with Mulliken algorithm.

The simulations of substrates docking in the active center of *Arthromyces ramosus* peroxidase (ARP) were performed with AutoDock 3.0 [16]. The crystal data of the complex of ARP with benzhydroxamic acid (HSR) [11] was downloaded from the Protein Data Bank. All water molecules in the active center of ARP were removed with the exception of a water molecule in the distal side of the heme. Atomic interaction energy grid maps were calculated with 0.25 Å grid spacing and 100 grid points forming 25 Å cubic box centered on the active site of peroxidases on heme side exposed to water. The space of the cubic box covered the active site of peroxidases and the space beyond. The electrostatic interaction energy grid used a distance-dependent dielectric function of Mehler-Solmajer. The docking was accomplished using Lamarckian genetic algorithm. The number of individuals in populations was set to 50. The maximum number of energy evaluations that the genetic algorithm should make was 250 000. Maximum number of generation was 27000. The number of the top individuals that are guaranteed to survive into the next generation was 1. Crossover rate and mutation rate were 0.02 and 0.80.

Acknowledgments

The authors express sincere thanks to H.-J. Deussen, K. Krikstopaitis and R. Lolck who have made synthesis and have determined the parameters of the compounds. We also thank P. Schneider for the help and support throughout the project and A.J. Olson for the supply of AutoDock 3.0 program.

References

1. Dunford HB: **Horseradish peroxidase: structure and kinetic properties.** *In: Peroxidases in Chemistry and Biology Volume 2 (Edited by Everse J, Everse K), CRC Press, Boca Raton, Ann Arbor, Boston,* 19911-25
2. Candeias LP, Folkes LK, Wardman P: **Factors controlling the substrate specificity of peroxidases: kinetics and thermodynamics of the reaction of horseradish peroxidase compound I with phenols and indole-3-acetic acids.** *Biochemistry* 1997, **36**:7081-7085
3. Krikstopaitis K, Kulys J, Pedersen AH, Schneider P: **N-substituted p-phenylenediamines as peroxidase and laccase substrates.** *Acta Chem.Scand* 1998, **52**:469-474
4. Ryabov AD, Goral VN, Ivanova EV, Reshetova MD, Hradsky A, Bildstein B: **Linear free-energy relationships and inverted Marcus region in the horseradish peroxidase-catalyzed oxidation of ferrocenes by hydrogen peroxide.** *J. Organ.Chem* 1999, **589**:85-91
5. Kulys J, Krikstopaitis K, Ziemys A: **Kinetics and thermodynamics of peroxidase-and laccase-catalyzed oxidation of N-substi-**

tuted phenothiazines and phenoxazines. *J. Biol.Inorg.Chem.* 2000, **5**:333-340
6. Sakurada J, Sekiguchi R, Sato K, Hosoya T: **Kinetic and molecular orbital studies on the rate of oxidation of monosubstituted phenols and anilines by horseradish peroxidase compound II.** *Biochemistry* 1990, **29**:4093-4098
7. Kulys J, Deussen H-J, Krikstopaitis K, Schneider P, Ziemys A: **N-aryl-N-hydroxy urethanes as peroxidase substrates.** *Mon.Chem* 2001, **132**:295-304
8. Kulys J, Deussen H-J, Krikstopaitis K, Lolck R, Schneider P, Ziemys A: **N-aryl hydroxamic acids as novel oxidoreductases substrates.** *Eur. J. Org. Chem.* 20013475-3484
9. Bixon M, Jortner J: **Electron transfer-from isolated molecules to biomolecules.** *In:Advances in Chemical Physics Volume 106, Part one (Edited by Jortner J, Bixon M)* 199935-202
10. Kunishima N, Fukuyama K, Matsubara H, Hatanaka H, Shibano Y, Amachi T: **Crystal structure of the fungal peroxidase from Arthromyces ramosus at 1.9 angstroms resolution: structural comparison with the lignin and cytchrome C peroxidases.** *J.Mol.Biol.* 1994, **235**:331-334
11. Itakura H, Oda Y, Fukuyama K: **Binding made of benzohydroxamic acid to Arthromyces ramosus peroxidase shown by X-ray crystallographic analysis of the complex at 1.6 Å resolution.** *FEBS Lett* 1997, **412**:107-110
12. Kohen A, Klinman JP: **Enzyme catalysis: Beyond classical paradigms.** *Acc. Chem. Res.* 1998, **31**:397-404
13. Henriksen A, Smith AT, Gajhede M: **Structures of the horseradish peroxidase c-ferulic acid complex and the ternary complex with cyanide suggest how peroxidases oxidize small phenolic substrates.** *J.Biol. Chem.* 1999, **274**:35005-35011
14. Jones P: **Roles of water in heme peroxidase and catalase mechanisms.** *J.Biol.Chem.* 2001, **276**:13791-13796
15. Frisch MJ, Trucks GW, Schlegel HB, Gill PMW, Johnson BG, Robb MA, Cheeseman JR, Keith T, Petersson GA, Montgomery JA, *et al*: **Gaussian 94, Revision E.1,** *Gaussian, Inc., Pittsburgh PA* 1995
16. Morris GM, Goodsell DS, Huey R, Olson AJ: **Distributed automated docking of flexible ligands to proteins: Parallel applications of AudoDock 2.4.** *J. Comp.-Aided. Mol.Des.* 1996, **10**:293-304